communications earth & environment

Article

https://doi.org/10.1038/s43247-024-01298-7

How, when and where current mass flows in Martian gullies are driven by CO_2 sublimation

Lonneke Roelofs[1,8] ✉, Susan J. Conway[2,8], Tjalling de Haas[1], Colin Dundas[3], Stephen R. Lewis[4], Jim McElwaine[5], Kelly Pasquon[2], Jan Raack[6,7], Matthew Sylvest[4] & Manish R. Patel[4]

Martian gullies resemble water-carved gullies on Earth, yet their present-day activity cannot be explained by water-driven processes. The sublimation of CO_2 has been proposed as an alternative driver for sediment transport, but how this mechanism works remains unknown. Here we combine laboratory experiments of CO_2-driven granular flows under Martian atmospheric pressure with 1D climate simulation modelling to unravel how, where, and when CO_2 can drive present-day gully activity. Our work shows that sublimation of CO_2 ice, under Martian atmospheric conditions can fluidize sediment and creates morphologies similar to those observed on Mars. Furthermore, the modelled climatic and topographic boundary conditions for this process, align with present-day gully activity. These results have implications for the influence of water versus CO_2-driven processes in gully formation and for the interpretation of gully landforms on other planets, as their existence is no longer definitive proof for flowing liquids.

Martian gullies are landforms consisting of an alcove, channel, and depositional apron. Since their discovery[1], they have sparked intense scientific debate because the conditions under which they evolved have far-reaching implications for the past and present-day water cycling on Mars, the presence of habitable environments, and future space exploration. Gullies have been hypothesized to form by the action of liquid water and brines[1–6], the effects of sublimating CO_2 frost[7–16], or a combination of these processes over time[17]. The morphometry, morphology, and sedimentology of Martian gully systems are indistinguishable from aqueous debris-flow systems on Earth[1,5,6,18]. However, their present-day activity[7,8,10,11,14–16,19–24] is incompatible with the low availability of stable liquid water under current Martian conditions[25,26] and the difficulty of melting pure water on the surface of Mars today[27].

Present-day activity occurs in the form of new lobate deposits on gully aprons[7,8], incision and formation of channels[10,16], and the movement of meter-scale boulders[8,16]. Early stages of gully initiation are also observed[28] as well the collapse of channel banks[12], demonstrating that the processes shaping and changing the gullies today are not merely modifying the pre-existing landforms, but are capable of actively shaping the landscape. Many contemporary flows deposit on substantially lower slopes than dry flows would[28]. Hence, these flows must have been fluidized[12]. The link between the timing of activity and the presence of CO_2 frost at the surface, suggests the involvement of sublimating CO_2[7–10,12–16]. The main hypotheses for CO_2-related mechanisms are; a) mixtures of sediment and CO_2 ice are fluidized by the gas flux induced by the sublimating CO_2[12,28,29], b) sediment is transported by pressurized flows underneath a translucent slab of CO_2 ice of which the base is sublimating due to solar radiation[30]. However, the requirement of slab ice means the latter mechanism is only applicable to Martian gullies at latitudes > 40°S where evidence for slab ice is observed[19,28].

Despite the growing body of evidence for CO_2 being involved in Martian gully flows, we face two major challenges. First, we do not have in-situ observations of activity in gullies. Therefore, it remains speculative if and how CO_2 sublimation drives granular flows and how this process can explain the observed morphologies. Second, our understanding of the

[1]Department of Physical Geography, Faculty of Geosciences, Utrecht University, Princetonlaan 8a, 3584 CB Utrecht, Netherlands. [2]Nantes Université, L'Université d'Angers, Le Mans Université, Laboratoire de Planétologie et Géodynamique, CNRS UMR 6112, 2 chemin de la Houssinière, BP 92205, Nantes 44322, France. [3]U.S. Geological Survey, Astrogeology Science Center, 2255 N. Gemini Dr., Flagstaff AZ 86001, USA. [4]School of Physical Sciences, The Open University, Milton Keynes, United Kingdom. [5]Department of Earth Sciences, Durham University, Durham, United Kingdom. [6]Institut für Planetology, Westfälische Wilhelms-Universität, Wilhelm-Klemm-Str. 10, 48149 Münster, Germany. [7]InnoCoding GmbH, Ludgeristraße 7/8, 48143 Münster, Germany. [8]These authors contributed equally: Lonneke Roelofs, Susan J. Conway. ✉e-mail: l.roelofs@uu.nl

climatic and topographic boundary conditions under which CO_2-driven granular flows could occur on present-day Mars is incomplete. On a global scale, we know that current activity occurs in places where CO_2 frost is present[7–10,12–16], but on a local scale, i.e. a specific gully on a specific crater wall, we cannot explain where gully activity occurs and where it does not. These challenges hamper our understanding of the evolution of the Martian surface, the past and present existence of liquid water on Mars, the habitability of the Martian surface, and the general influence of liquid- versus sublimation-driven processes on planetary surfaces.

Here, we present a new framework for CO_2-driven granular flows on Mars that we validate with the first physical tests of granular flows fluidized by sublimating CO_2 under Martian atmospheric conditions. Furthermore, we schematize this framework into a climate model, of which we compare the results to present-day gully activity on Mars.

Conceptual framework for Martian CO_2 driven granular flows

The basis of our framework considers a Martian gully system in winter. Due to the complex topography of the gully, there are illuminated slopes and shaded slopes within the gully. This results in local temperature differences, with some slopes at temperatures at the CO_2 frost point and others above. When a slope failure occurs, CO_2 frost can come into contact with substantially warmer material. How this initial slope failure occurs is beyond the scope of this research, but could include dry raveling, rock fall[31–33], CO_2 sublimation-induced slumping[34,35], meteor impacts, or marsquakes. The higher temperature of the warmer material provides an energy source for sublimation of the CO_2, possibly aided by heat produced by the release of kinetic energy during movement[19]. The gas flux, induced by the sublimation, depends on the ratio between the density of CO_2 ice and gas. In the thin Martian atmosphere (~800 Pa), the gas flux created by CO_2 sublimation is >100 larger than under Earth's atmosphere and thus likely sufficient to fluidize sediments[12,36]. As long as the gas production produces sufficient pore pressure, defined by Darcy's law, to reduce intergranular friction, movement can occur[12,34–36]. One can think of two mechanisms in which enough CO_2 frost can be supplied for fluidization to sustain a granular flow over long distances and low gradients; 1) a loose mixture of sediment and CO_2 frost tumbles or falls on top of a warmer surface, where sublimation is induced when the CO_2 touches the warmer surface, which fluidizes the mixture (Fig. 1a). Every timestep only a small percentage of the CO_2 in the mixture touches the warmer surface and sublimates, enabling the fluidization of the material over a long distance until all CO_2 has sublimated. And 2) warmer sediments ravel, slump, or fall on top of a CO_2 frosted surface, inducing the sublimation of this frost and thus the fluidization of the sediment (Fig. 1b). The flow can continue as long as frost is present along its path, and the flow itself contains sufficient heat. Both mechanisms can be illustrated by specific examples on Mars. Mechanism 1 is illustrated with an example based on observations of Matara crater dune field (Fig. 2a–e) that show discrete failures in frost-coated slopes neighbouring defrosted slopes[23]. Mechanism 2 is illustrated with an example based on observations in Selevac crater (Fig. 2f–h) showing failures in ice-free regolith that caused

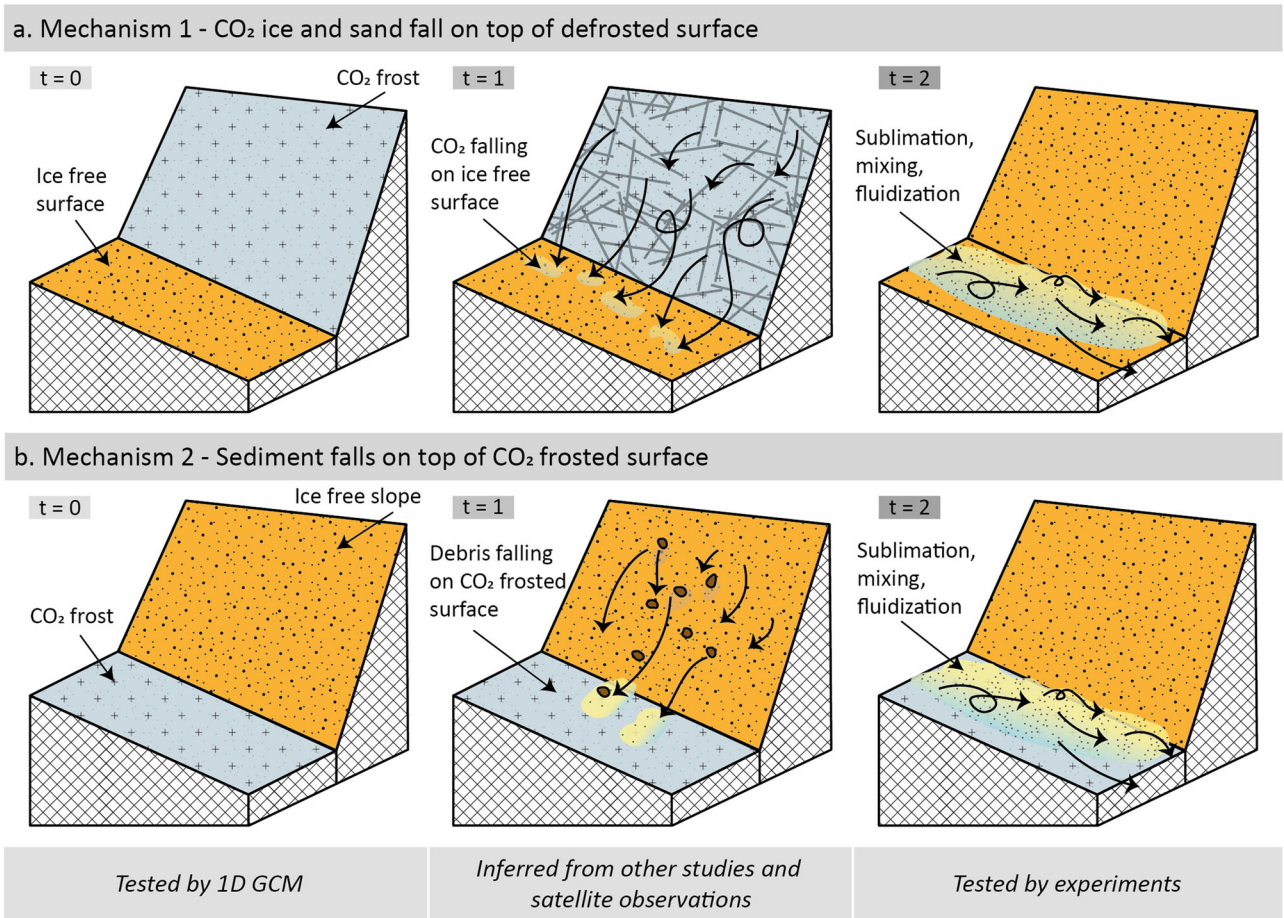

Fig. 1 | Schematic of the two tested mechanisms for gully activity. The block diagrams display a small part of the gully system, i.e., two neighbouring slope facets. **a** Mechanism 1 – Failures in frost-coated slopes lead to mixing of CO_2 ice and warmer sediment, sublimation of the CO_2 ice and ultimately fluidization of the sediment-ice mixture (see also Fig. 2a–e). **b** Mechanism 2 – Dry mass-movement of sediment onto a frosted surface, which leads to mixing and sublimation of the frost, and ultimately, fluidization of the sediment-ice mixture (see also Fig. 2f–h). Note that the model runs in this research test the conditions at $t = 0$, whereas the experiments test the physical feasibility of the process at $t = 2$.

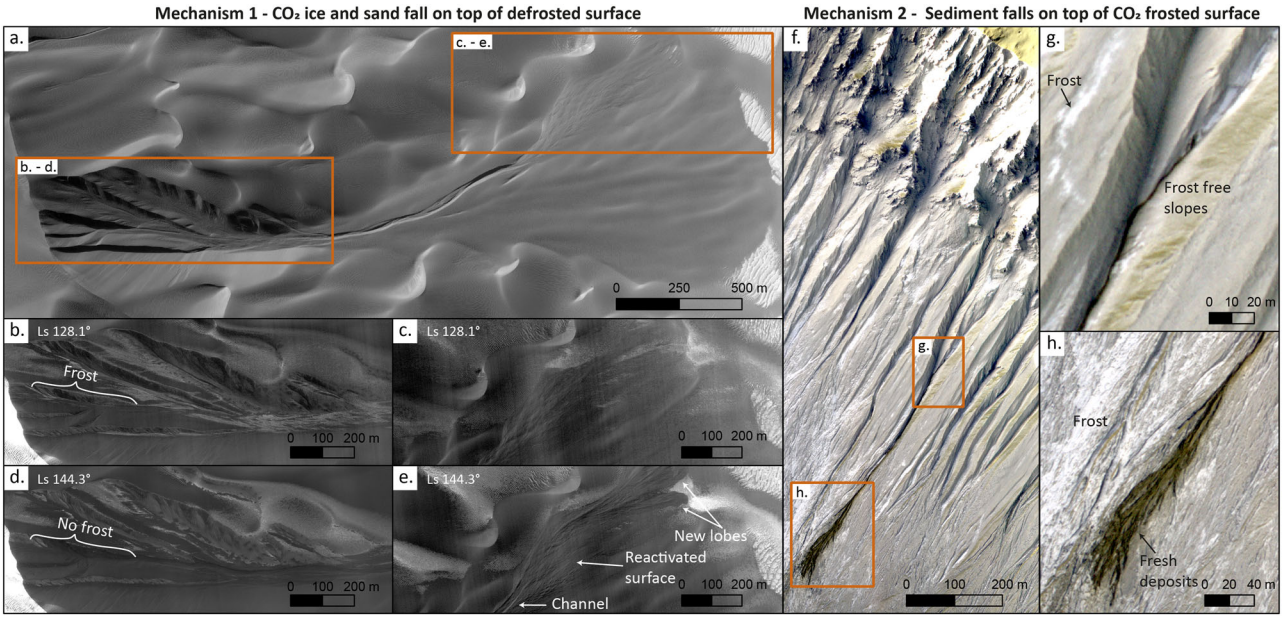

Fig. 2 | Examples of the two mechanisms for gully activity due to CO_2 ice sublimation on Mars. Images were taken by HiRISE. **a**–**e** Gully system on Matara crater dune field (**a** PSP_006648_1300) depicting mechanism 1: failures in frost coated slopes lead to mixing of ice and sediment, CO_2 sublimation, fluidization and sediment transport (**b**–**c** ESP_036488_1300 and **d**–**e** ESP_036910_1300). **f**–**h** Gully system in Selevac crater (ESP_027567_1425) depicting mechanism 2; an ice-free slope-failure (**g**) falls on top of a frosted surface (**h**), causing CO_2 sublimation, fluidization and sediment transport. Illumination from the upper left.

warmer sediment to fall on top of a CO_2-frosted surface causing a dark deposit.

Our proposed mechanisms imply that for the formation of CO_2 driven granular flows in gullies, three conditions have to be met, in addition to the presence of unconsolidated granular material available for transport;

- The presence of steep slopes where initial mass movements can occur.
- Slopes that are cold enough to host CO_2 frost.
- Neighbouring slopes above the CO_2 frost point to provide the heat energy needed to induce the sublimation of CO_2 frost after the initial mass-movement.

To test the two proposed mechanisms, we combine the first flume experiments of granular flows fluidized by sublimating CO_2 ice under Martian conditions, with a 1D numerical atmosphere and subsurface column model that explores the spatial and temporal distribution of the coexistence of CO_2 frosted and adjacent defrosted surfaces on Mars. For the experiments, we use a small-scale flume set-up inside an environmental chamber to simulate CO_2-driven granular flows under Martian atmospheric pressure. The flume design is informed by four decades of experimental research on Earth debris flows[37–41] (see Methods 5). For the 1D climate modelling, we simulate the temperature and possible condensation of CO_2 frost on multiple steeply sloping surfaces, typical of the source areas of Martian gullies at a range of latitudes. Steep slopes occur on small (<1 km) horizontal scales that are not resolved by 3D global atmospheric models (spatial resolution is typically ~100 km).

Results

Does it flow? Experimental CO_2-driven granular flows

To test our two proposed mechanisms for CO_2-driven granular flows on Mars, we performed flume experiments in the Mars chamber at the Open University (UK) (see Methods 5 for details of the set-up). Here, we present four experiments and four duplicates (Supplementary Notes 1, Supplementary Fig. 2). Videos of the experiments are available in the Supplementary Videos 1–15.

The first experiment tested mechanism 1 (Fig. 3a–c). In this experiment, a mixture of sand and CO_2 ice flowed out into a heated flume with a slope of 30°. The flume bottom was heated up to 20 °C, to simulate the maximum modelled temperature difference between the CO_2 ice and the neighbouring slope (~ 140 °C) and ensure a surplus of energy available for CO_2 sublimation. We used an initial CO_2 ice weight of 0.3 kg. To remain in thermal equilibrium, half of the CO_2 ice sublimated before the experiment during the lowering of the atmospheric pressure in the chamber. As a result, 0.15 kg of CO_2 ice was left for sublimation during the experiment against 1 kg of sediment. The second experiment tested mechanism 2 (Fig. 3d–f). In this experiment, we let dry sand (20 °C) flow over a 2 mm thick layer of crushed CO_2 ice (−120 °C). We further performed two reference experiments; one under Martian atmospheric pressure without CO_2, and one under Earth atmospheric pressure (1020 hPa) with CO_2.

The two experiments testing the proposed CO_2-driven mechanisms show strongly fluidized flows, with frontal flow velocities of >2 m s^{-1} (Fig. 3a, d), multiple surges (Supplementary Fig. 1a, b), increased flow depth (Supplementary Fig. 1a, b), and elongated, depositional lobes (Fig. 3c, f). Small levees are observed within the depositional lobes (Fig. 3c), implying the occurrence of grain segregation and formation of complex velocity profiles within the flows. With both tested scenarios, the increased mobilisation of the sediment in the chute is sustained until all sediment has left the chute. Fluidization is most severe when testing mechanism 2, when sediment flows over a layer of CO_2 ice; sand grains are ejected upwards and a dust cloud forms as a result of the increased gas pressure generated from the sublimating CO_2 ice (Fig. 3d). However, this intense mobilisation of the sediment quickly halts when the mixture reaches the outflow plain and loses momentum. This contrasts the more prolonged movement of sediment on the outflow plain under the conditions of mechanism 1, when CO_2 ice is present in the sediment mixture from the start (Fig. 3b, c).

In the experiment without CO_2 ice under Martian atmosphere, and the experiment with CO_2 ice under Earth's atmosphere, fluidization of the sediment does not occur (Fig. 3g–l, Supplementary Fig. 1c, d). This highlights that the combination of CO_2 ice sublimation and the low Martian atmospheric pressure is key in the increased mobilization of sediment. For both CO_2-driven mechanisms, the gas flux into the flow induces a pore pressure which reduces friction between the grains. In the fully supported case, there will be no significant friction and the drag will be set by viscous and/or turbulent stresses leading to much higher flow velocities and run-out. Furthermore, dimensional scaling analysis shows that under Martian

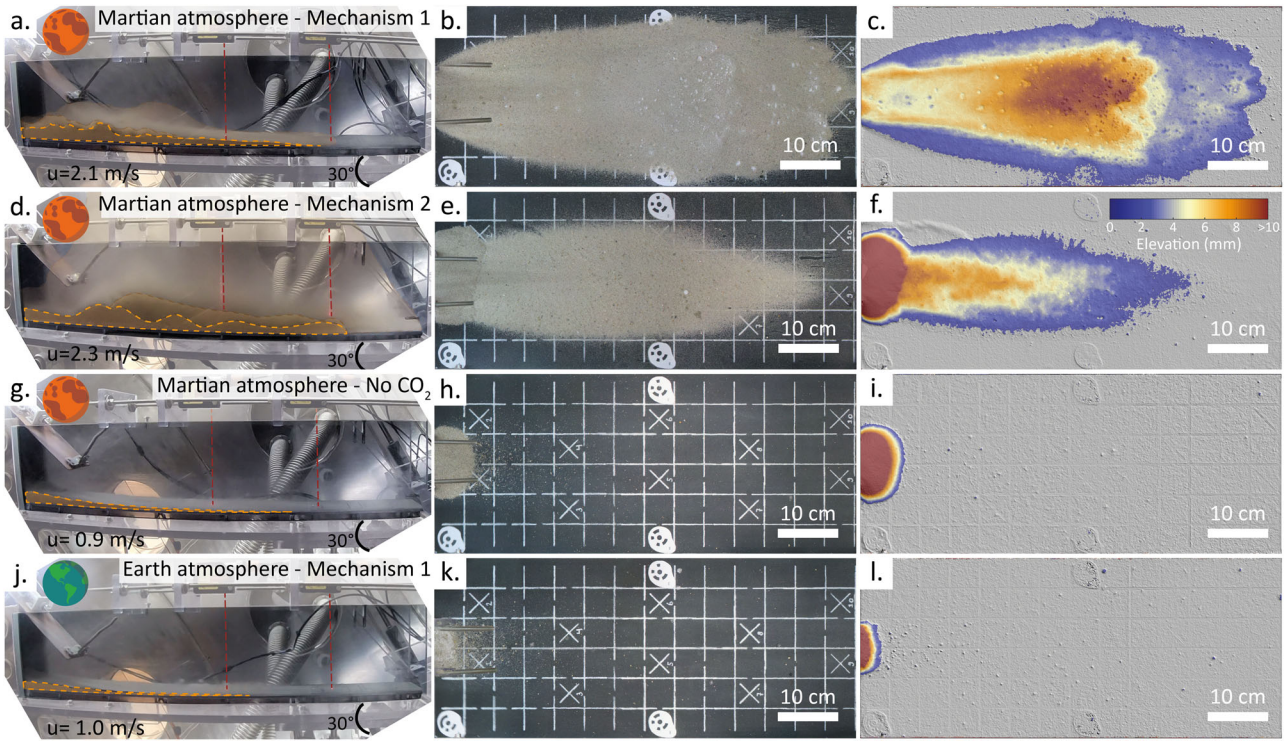

Fig. 3 | Overview of the experimental results. The first column shows photos of the granular flow in the chute (70 cm long) during the experiments, accompanied by the measured flow velocities (u). The locations of the laser distance sensors are indicated by red dotted lines. The orange dotted lines indicate shifts in flow density. The second column depicts the orthomosaics of the final deposits. The third column shows the digital elevation models of the final deposits. The first row (**a**–**c**) depicts the experiment testing mechanism 1, where a mixture of sand and CO_2 ice is released into the chute. The second row (**d**–**f**) shows the experiment testing mechanism 2, where sand is released into a chute covered with CO_2 ice. **g**–**i** Highlight the results of the experiment under Martian pressure without CO_2 ice. **j**–**l** The results of the reference experiment under Earth's atmosphere, where a mixture of sand and CO_2 ice were released into a heated chute.

gravity only 0.38 of the volume flux of CO_2 is needed for fluidization compared to Earth (see Methods 5.4). This implies that because the CO_2-driven mechanisms work in our experiments under Earth's gravity, fluidization would be even more effective under Martian gravity.

For the first time, these experiments provide direct evidence that CO_2 sublimation can fluidize, and sustain, granular flows under Martian atmospheric conditions, both where sediments and CO_2 ice are mixed and where dry sediment flows over a layer of CO_2 ice. The experiments, however, do not address the boundary conditions enabling these flows. We tackle this with a 1D atmospheric model below that determines where and when appropriate conditions on Mars can occur.

Relation between recent activity, proposed mechanisms, and climatic boundary conditions

To test whether, where, and when the conditions for the two mechanisms can be met on present-day Mars, we used a 1D atmospheric model (the 1D version of the Mars PCM, developed at LMD/IPSL) to predict the possible locations and timing of the boundary conditions needed for the two mechanisms. We then determined if the predicted locations coincide with the locations of present-day gully activity. The 1D atmospheric model uses the same physical schemes as the 3D version of the Mars PCM[42,43], with the solar irradiance scheme for slopes activated[44]. For more information on the model see Methods 5.5.

We examined the two mechanisms for gully activity as follows; the first scenario, representing mechanism 1, requires a sloping frosted surface and an adjacent defrosted surface with a different slope, and for this study, we assumed flat as a reasonable starting point for the defrosted slope. The second scenario, representing mechanism 2, requires two slopes with a similar orientation, yet differing thermal inertia (TI) properties. This is caused by the difference between bedrock and unconsolidated sediment, allowing CO_2 frost to persist for longer on unconsolidated material[45] (for more details see Methods section 5.5). Our model does not directly account for the presence of subsurface water ice[45], the effects of CO_2 ice on the surface nor the effect of incident infrared flux on the slope energy budget[46]. These parameters influence the surface temperature and thus the deposition of ice on the surface. Therefore, in tuning the modelled presence of CO_2 to match the observations of frost, we needed to use a higher TI than usually used by other Martian climate modelling studies[45,46]. For more detailed information and sensitivity analysis on the effect of different TI's we refer to the Supplementary Notes 2.

Our model results (Fig. 4) detail the temperature difference between the two surfaces. Temperature differences are only shown for the time and locations for which the reference surface is at the CO_2 frost temperature, i.e., CO_2 is present, and the other surface is above CO_2 frost temperature. For mechanism 1, this is the temperature difference between a pole-facing steep frosted surface (35° slope) and a flat surface without frost (Fig. 4a). Both modelled surfaces have a TI of 1000 J m^{-2} s$^{1/2}$ K^{-1}. For mechanism 2 this is the temperature difference between 35° slopes with a high TI (1250 J m^{-2} s$^{1/2}$ K^{-1}), associated with bedrock on Mars[47,48], and a neighbouring 15° slope with a lower TI (750 J m^{-2} s$^{1/2}$ K^{-1}), presented here for a south-facing orientation (Fig. 4b) (for additional model runs with different TI's, slope angles and slope cardinal directions see Supplementary Notes 3 and Supplementary Figs. 4–6).

The model results suggest that frosted slopes can co-occur with warm slopes for both mechanisms at the same latitude and around the same time during the Martian year (described in solar longitude). The observed present-day activity in Martian gullies, presented by the lines in Fig. 4, falls within the valid temperature-difference envelope given by the model scenarios. This is especially true for mechanism 1 and for south-facing slopes within mechanism 2. Furthermore, our model results correlate with observations of CO_2 frost on steep slopes[28,45] (Supplementary Notes 3).

Our model predicts that some of the gully population should be inactive at present, including northern hemisphere gullies at latitudes lower

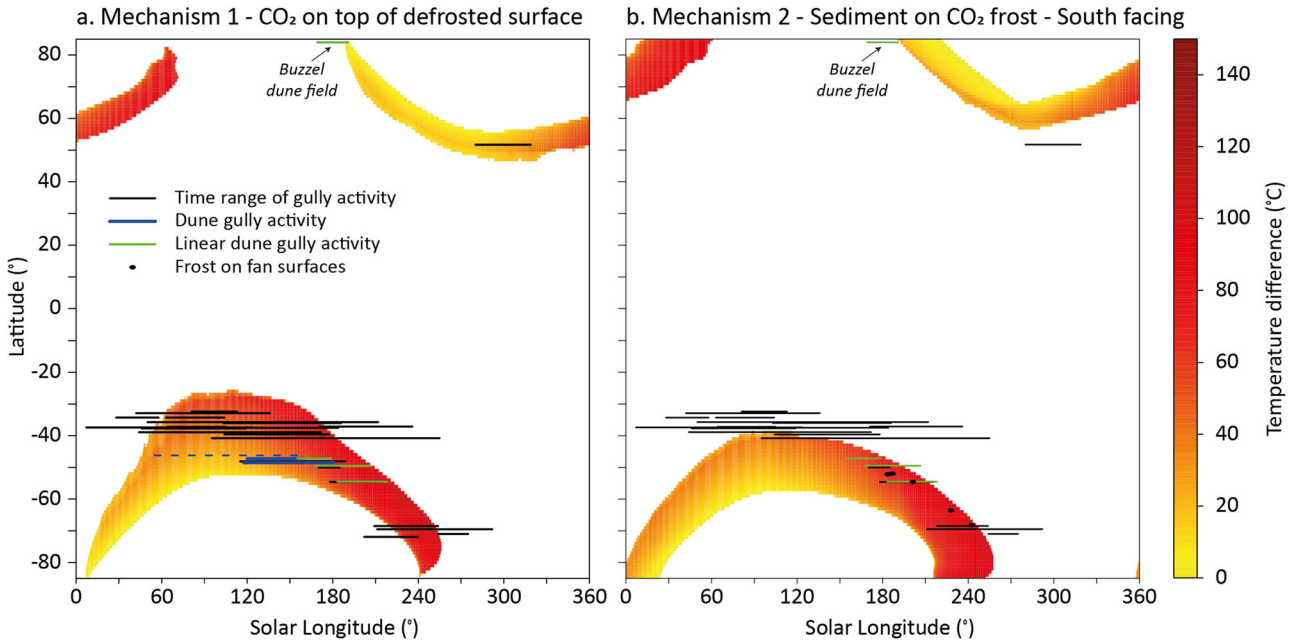

Fig. 4 | Climate model results with observed gully activity superimposed. Colour indicates the maximum daily temperature difference between frosted and unfrosted surfaces for (**a**) mechanism 1 and (**b**) mechanism 2 for south-facing slopes for different latitudes over a Martian year (depicted in Solar Longitude). Temperature differences between slopes are projected as different colours. Timing and location of recent gully activity are given in black[14,24], activity in dune gullies by blue lines and in linear gullies by green lines[21], observed ongoing activity is highlighted by dashed lines. The green line in the Northern hemisphere is an alcove failure on Buzzel dune field[57]. Black dots are observations of frost on gully fans from HiRISE and CaSSIS[28].

than ~ 50° and all but the poleward-most equator-facing gullies in both hemispheres (Fig. 4). These predictions are to date supported by a lack of observed activity in gullies in these geographical zones. The only exception is activity observed on some equator-facing gullies. This activity could have been caused by the presence of pole-facing slope facets which can host CO_2 ice[19] or by a difference in thermal inertia in partly defrosted alcoves, as seen in Sisyphi Cavi[11,24].

Implications for Martian gullies and other planetary landforms

The combined results of our experiments and models reveal that liquid water is not required to explain present-day activity in Martian gullies and that CO_2 sublimation processes can explain most of our observations in active Martian gully systems today, under the condition that enough thermal energy is available for the sublimation of CO_2 ice. In our study, the energy needed for CO_2 ice sublimation is presumed to come from heated slopes that are at temperatures far above the CO_2 frost temperature (up to 20 °C in our simulations). experiments specifically prove that sublimation of CO_2 can mobilize, fluidize, and transport sediment as long as CO_2 ice in the flow mixture or the bed continues to sublimate. The deposit morphology in our experiments contains key features that are also observed in Martian gully deposits, like levees and lobes. This indicates similarity in flow dynamics between our experimental CO_2-driven granular flows and experimental and field scale granular flows on Earth, both debris flows[38–41] and pyroclastic density currents[49,50]. The results from the 1D model further indicate that the location and timing of the climatic boundary conditions of the proposed CO_2 fluidization mechanisms coincide with observations of present-day gully activity on Mars.

Our findings have implications for the search for potential liquid water on Mars, as well as the interpretation of landforms on other planetary bodies, including gullies on Vesta[51] and Mercury[52]. For Mars, substantiating sublimation as an important sediment transport process in gullies today shows we possibly need no to less water to explain our observations than previously thought, which can have implications for the amount of water thought to have existed throughout the Amazonian on Mars. To quantify this; it has been estimated that to explain geomorphic activity in gullies in Istok crater with flowing water, a minimum equivalent water layer of 1 mm across all alcoves is needed, with estimates up to 50 mm of water for larger flows[6]. Other estimates predict that at least 0.15 km^3 of water has flowed across the surface of Mars to carve the gully systems we observe today[53]. As the water inventory of Mars crosses several research domains, from atmospheric sciences to astrobiology, our findings could cascade into many different fields. Definitive proof of the formation process of Martian gullies can only be provided by true in-situ observations of present-day activity combined with detailed sedimentological analysis of their deposits. However, as both of these are currently unachievable, we believe it is wise to be cautious about assuming a water-driven past for the Martian gullies and to consider the possibility of CO_2-related processes being involved in their formation. For other planetary bodies with low atmospheric pressures, our results imply that the existence of gully-like systems is no longer a direct proof of flowing liquids as these landforms could as well be formed, or at least be influenced, by sublimation-driven processes. Therefore, our findings could be the start of a fundamental reinterpretation of extra-terrestrial landforms. This will affect hypotheses on potential extraterrestrial habitable environments and predictions on the availability of resources for future exploration of the Solar System.

Methods

Experimental flume set-up and Mars chamber

The experiments were performed in a small-scale flume in the Mars chamber at the Open University in Milton Keynes, United Kingdom. The Mars chamber is a cylindrical chamber with a diameter of 0.9 m and length of 1.8 m (see Fig. 5) that can be depressurized to Martian atmospheric pressure. The desired pressure can be set and is automatically regulated, but the depressurization rate is manually controlled by opening the valve to the pump.

The design of the flume inserted into the chamber was based on set-ups for simulating terrestrial debris flows on a small scales[39–41,54]. These set-ups consist of a sediment reservoir, from which the mass flow is released, a steeper narrow chute for studying flow properties, and an outflow plain to

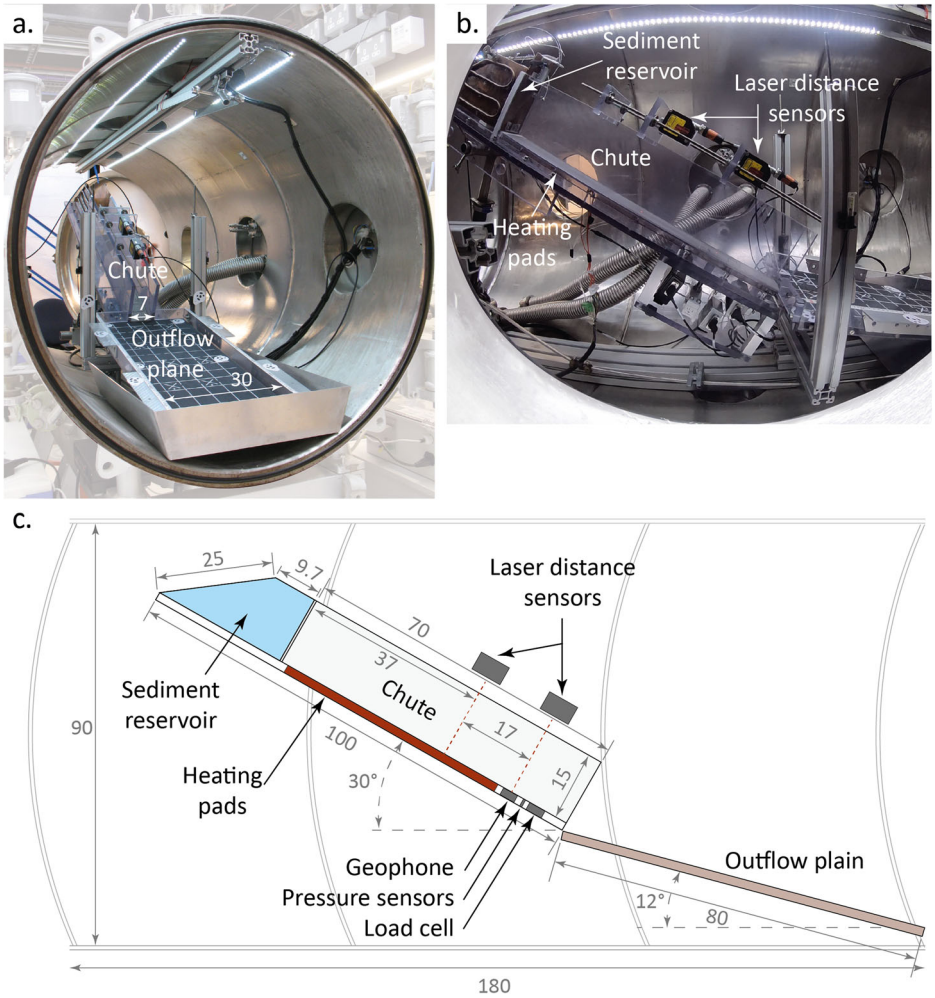

Fig. 5 | Mars chamber and flume set-up. a A frontal view of the flume in the Mars chamber. **b** A side view of the flume in the chamber right before an experiment. **c** Technical sketch of the flume. All dimensions are given in cm. Important flume elements and sensors are indicated with arrows and descriptions.

study flow deposits. The flume used here consisted of a reservoir with a trap door (2.07 L), a steep narrow chute (7 × 15 × 70 cm), and an outflow plain (30 × 80 cm), see Fig. 5. The slope of the chute was kept at 30° and the slope of the outflow plain at 12°. Heating pads were installed at the bottom of the chute to regulate the temperature of the chute floor. To simulate natural roughness, the aluminum bottom of the chute was sandblasted, and the outflow plain was covered with sandpaper. Above the chute two OADM 20U2480/S14C laser distance sensors were installed at 0.37 m and 0.54 m from the top of the chute (see Fig. 5). They measured with a frequency of 10 000 Hz and have sub-mm accuracy during the passage of the flow.

Flume experiments

Four key experiments were performed to test the two mechanisms discussed in the main text of the paper. Three experiments were conducted under Martian atmospheric pressure and one experiment was executed under Earth atmospheric pressure (see section 3.1). To ensure repeatability, all experiments were repeated. For results of the duplicate experiments see Supplementary Notes 1. The first experiment tested mechanism 1, where a mixture of CO_2 ice and sediment flowed over a non-frosted surface that was kept at a constant temperature of 20 °C, to simulate the maximum modelled temperature difference between the CO_2 ice and the neighbouring slope (see Fig. 4 and Section 3). The second experiment tested mechanism 2, where warm sediment (20 °C) comes into contact with a CO_2 frosted surface. The third experiment was the reference experiment without CO_2 ice under Martian atmospheric pressure. In this experiment, only sediment was released from the reservoir. The fourth experiment was similar to the experiment testing mechanism 1, but now performed under Earth atmospheric pressure. For all experiments, 1 kg of sediment was used. The sediment used in the experiments consisted of a moderately sorted sub-rounded fluvial sand, with a median grain size of 310 μm. The sediment was selected because of its fine to medium grain size and its broad grain size distribution that minimizes gas permeability relative to a mono-disperse sand, and thus slows down the gas escape rate.

When CO_2 ice was mixed with the sediment we used an initial CO_2 ice weight of 0.3 kg. To remain in thermal equilibrium, half of the CO_2 ice sublimated before the experiment during the lowering of the atmospheric pressure in the chamber. As a result, 0.15 kg of CO_2 ice was left for sublimation during the experiment. In the experiment where sediment flowed over a frosted surface, a 2 mm thick layer of crushed CO_2 ice was placed on the bottom of the chute. Lowering of the layer thickness during depressurisation of the chamber was minimal.

Experimental procedure

The procedure for executing an experiment consisted of the following steps. The CO_2 ice was manually crushed to a median grain size similar to the sand. The ice was then mixed with the sediment while monitoring the weight. The latter was essential because the CO_2 ice sublimated as it cooled the sediment. When the desired CO_2 weight was reached the mixture was loaded into the reservoir. For the experiments conducted under Martian atmospheric pressure, the chamber was subsequently closed and depressurized to 800 Pa in 10–12 minutes. When an atmospheric pressure of 800 Pa was reached, the pressure was stabilised and the trap door of the reservoir was opened letting the mixture flow out. For the experiment under Earth atmospheric pressure, the chamber was closed but not depressurized. 12 minutes after loading the

sediment, the mixture was released. After the experiment, the chamber was depressurized in 4–5 min. The chamber was opened and 40-50 photos were taken of the deposit with a Canon PowerShot A640 for multi-view photogrammetry. DTMs and orthophotos of the surface were created with a pixel size of 300 μm using Agisoft Metashape Professional (results shown in Fig. 3 and Supplementary Fig. 2).

Scaling for gravity in flume experiments

In our experiments we did not directly scale for the weaker gravity of Mars relative to Earth. However, this difference can be understood theoretically by dimensional analysis. The most important driver of CO_2 driven flows is the sublimation of the CO_2 frost, which is independent of gravity due to CO_2 being the dominant gas[55]. The effect of gravity comes into the equation in the form of the weight of the particles in the flow. The extent to which the flow is suspended is given by a non-dimensional group, which describes the ratio of the Darcy pressure $hq\nu/d^2$ to the weight of the flow $hg\rho_s$;

$$\frac{hq\nu}{hg\rho_s d^2} = \frac{q\nu}{g\rho_s d^2}. \quad (1)$$

where is ρ_s is the density of the solid material in kg m^{-2}, where h is the flow depth in m, q is the volume flux of CO_2 in m s^{-1}, ν is the dynamic viscosity of the CO_2 gas in kg m^{-1} s^{-1}, g is the gravitational acceleration and d is the grain diameter in m s^{-2}. ν is the same for our experiments and Mars. g is different but this can be accommodated by adjusting the grain diameter d, the solid density ρ_s or sublimation velocity q.

This shows that under Martian gravity only 0.38 of the volume flux of CO_2 is needed compared to Earth to fluidize a flow. In the practical sense, this means that under Martian gravity, if we were to repeat the experiment testing mechanism 1, we would be able to decrease the amount of CO_2 used to fluidize 1 kg of sediment over the length of our flume to 58 g at the start of an experiment (volume fraction of 5.8×10^{-2}). This is close to the volume fraction range, 2×10^{-2} – 2×10^{-5}, predicted to be needed for recent gully flows in Hale crater[12], especially if you account for the lack of replenishment of CO_2 ice in our experimental set-up of mechanism 1.

1D column version of the Mars Planetary Climate Model

The 1D atmosphere and subsurface column model uses physical schemes extracted from the Mars Planetary Climate Model (PCM)[42,43], with the solar irradiance scheme for slopes activated[44] to simulate surface temperature on slopes of 0°, 15° and 35°, oriented to face north, south, east or west for all latitudes (at 1° intervals). We used current orbital conditions: orbital obliquity of 25°, and perihelion at L_s 251° (in southern summer). Mars receives 45% more insolation at perihelion than aphelion due to its eccentric orbit[26]. We fixed the surface pressure to 610 Pa (we also performed tests at 500 and 800 Pa, which produced no noticeable difference in our results). When CO_2 ice condenses or sublimates this means that the 1D atmospheric column does not conserve mass. This is true in reality for any single location; additional atmospheric mass and heat, including the latent heat released as more mass becomes available to condense, can be advected into a region horizontally, an effect that can only be represented correctly in a global 3D model. Where the surface pressure in the 1D model is allowed to alter, polar night can result in an unrealistically low surface pressure as the whole local atmosphere column freezes.

The 1D version of the model applies the same set of physical submodels as the Mars PCM. It uses astronomical parameters to calculate the total incoming solar radiation at the top of the atmosphere, which drives the atmospheric system. In computing the radiative transfer through the atmosphere the model accounts for absorption, emission, and scattering by CO_2 gas and dust, over a range of wavelengths from ultraviolet to infrared. Small-scale dynamical processes of the atmosphere, such as turbulent diffusion and convection, are parameterized. The model accounts for the condensation and sublimation of CO_2 at the surface and contains a soil model which describes the thermal inertia (TI) of the ground, with 18 subsurface layers, and its albedo and radiative flux balance at the surface.

We used three soil TIs of 750, 1000, and 1250 J m^{-2} s$^{1/2}$ K^{-1} (also referred to as thermal inertia units, tiu) as is realistic for an ice-free soil, a moderately water ice-rich soil and an ice-rich soil at the latitudes with gullies[45]. We used a bare soil albedo of 0.2[56] (tests at 0.1 and 0.05 produced no noticeable difference in our results). For two specific TIs and slope configurations, the results are presented in the main body of the paper, whereas the results with the other TIs can be found in the Supplementary Notes - 3. We would like to highlight that the TIs used in this study are high in comparison to those usually used by Martian climate modelling studies[45,46]. Our model does not directly account for the presence of subsurface water ice[45], the effects of CO_2 ice already present on the surface, or the effect of incident infrared flux on the slope energy budget[46]. However, the correct prediction of the locations and timings of CO_2 frost and the temperature of the other hillslopes is essential to test our mechanisms. To get the modelled presence of CO_2 to match the observations, we used a relatively high surface TI in our model set-up. We based the TIs used in the main part of the manuscript on a model tuning step where we sought to match the predicted presence of CO_2 frost on north and south-facing slopes of 35° (see Supplementary Notes 2) to observations of frost on steep slopes[28,45].

We performed model runs two Mars years in duration where the surface temperature was recorded every half hour at every location. Only data from the second Mars year are used for analysis. For mechanism 1, we calculated the temperature difference between frosted slopes at 35° oriented poleward with adjacent flat areas, both with a TI of 1000 J m^{-2} s$^{1/2}$ K^{-1}. Frosted slopes adjacent to defrosted flat terrain only occur on pole-facing orientations. For mechanism 2, we calculated the maximum temperature difference between triplets of slopes at 35° slope oriented N, S, E, and W with a TI of 1250 J m^{-2} s$^{1/2}$ K^{-1} compared to frosted slopes at 15° slope with a TI of 750 J m^{-2} s$^{1/2}$ K^{-1}. For each orientation, the triplet comprised the central orientation and its two immediate neighbours. In Fig. 4 temperature differences are only plotted if the lower temperature is at the CO_2 condensation point, i.e., if CO_2 ice is present on one of the surfaces.

Data availability

In this study, we used data collected during the experiments, including digital elevation data and sensor data of flow dynamics, and we used output data of the 1D version of the Mars PCM. All this data is stored on YODA, the online repository of Utrecht University. The data is accessible under this link[58]: • https://doi.org/10.24416/UU01-SVJJB8 • https://public.yoda.uu.nl/geo/UU01/SVJJB8.html.

Received: 29 August 2023; Accepted: 1 March 2024;
Published online: 13 March 2024

References

1. Malin, M. C. & Edgett, K. S. Evidence for recent groundwater seepage and surface runoff on Mars. *Science* **288**, 2330–2335 (2000).
2. Costard, F., Forget, F., Mangold, N. & Peulvast, J. P. Formation of recent martian debris flows by melting of near-surface ground ice at high obliquity. *Science* **295**, 110–113 (2002).
3. Knauth, L. & Burt, D. M. Eutectic brines on Mars: Origin and possible relation to young seepage features. *Icarus* **158**, 267–271 (2002).
4. Christensen, P. R. Formation of recent Martian gullies through melting of extensive water-rich snow deposits. *Nature* **422**, 45–48 (2003).
5. Conway, S. J. et al. The indication of martian gully formation processes by slope–area analysis. *Geolog. Soc., London, Special Publ.* **356**, 171–201 (2011).
6. de Haas, T. et al. Earth-like aqueous debris-flow activity on Mars at high orbital obliquity in the last million years. *Nat. Commun.* **6**, 1–6 (2015).
7. Diniega, S., Byrne, S., Bridges, N. T., Dundas, C. M. & McEwen, A. S. Seasonality of present-day Martian dune-gully activity. *Geology* **38**, 1047–1050 (2010).
8. Dundas, C. M., McEwen, A. S., Diniega, S., Byrne, S. & Martinez-Alonso, S. New and recent gully activity on Mars as seen by hirise.

Geophys. Res. Lett. **37**, 1–5 (2010). https://agupubs.onlinelibrary.wiley.com/doi/abs/10.1029/2009GL041351.
9. Dundas, C. M., Diniega, S., Hansen, C. J., Byrne, S. & McEwen, A. S. Seasonal activity and morphological changes in martian gullies. *Icarus* **220**, 124–143 (2012).
10. Dundas, C. M., Diniega, S. & McEwen, A. S. Long-term monitoring of martian gully formation and evolution with mro/hirise. *Icarus* **251**, 244–263 (2015).
11. Raack, J. et al. Present-day seasonal gully activity in a south polar pit (Sisyphi Cavi) on Mars. *Icarus* **251**, 226–243 (2015).
12. de Haas, T. et al. Initiation and flow conditions of contemporary flows in martian gullies. *J. Geophys. Res.: Planets* **124**, 2246–2271 (2019).
13. Khuller, A. R., Christensen, P. R., Harrison, T. N. & Diniega, S. The distribution of frosts on Mars: Links to present-day gully activity. *J. Geophys. Res.: Planets* **126**, e2020JE006577 (2021).
14. Dundas, C. M., Conway, S. J. & Cushing, G. E. Martian gully activity and the gully sediment transport system. *Icarus* **386**, 115133 (2022). https://www.sciencedirect.com/science/article/pii/S0019103522002408.
15. Pasquon, K. et al. Insights into the interaction between defrosting seasonal ices and gully activity from CaSSIS and HiRISE observations in Sisyphi Cavi, Mars. *Planetary Space Sci.* **235**, 105743 (2023).
16. Sinha, R. K. & Ray, D. Morphological changes currently occurring in sand-filled gully channels on Mars: Implications for the role of substrates inside channels. *Icarus* **390**, 115334 (2023).
17. Dickson, J. L. et al. Gullies on Mars could have formed by melting of water ice during periods of high obliquity. *Science* **380**, 1363–1367 (2023).
18. Dickson, J. L. & Head, J. W. The formation and evolution of youthful gullies on Mars: Gullies as the late-stage phase of Mars' most recent ice age. *Icarus* **204**, 63–86 (2009).
19. Dundas, C. M. et al. The formation of gullies on Mars today. *Geolog. Soc., London, Special Publ.* **467**, 67–94 (2017).
20. Jouannic, G. et al. Morphological characterization of landforms produced by springtime seasonal activity on Russell crater megadune, Mars. *Geolog. Soc. London, Special Publ.* **467**, 115–144 (2018).
21. Pasquon, K., Gargani, J., Massé, M. & Conway, S. J. Present-day formation and seasonal evolution of linear dune gullies on Mars. *Icarus* **274**, 195–210 (2016).
22. Pasquon, K. et al. Are different Martian gully morphologies due to different processes on the Kaiser dune field? *Geolog. Society, London, Special Publ.* **467**, 145–164 (2018).
23. Pasquon, K. et al. Present-day development of gully-channel sinuosity by carbon dioxide gas supported flows on mars. *Icarus* **329**, 296–313 (2019).
24. Raack, J. et al. Present-day gully activity in Sisyphi Cavi, Mars – flow-like features and block movements. *Icarus* **350**, 113899 (2020).
25. Hecht, M. H. Metastability of liquid water on Mars. *Icarus* **156**, 373–386 (2002).
26. Richardson, M. I. & Mischna, M. A. Long-term evolution of transient liquid water on Mars. *J. Geophys. Res.: Planets* **110**, E03003 (2005).
27. Schorghofer, N. Mars: Quantitative evaluation of crocus melting behind boulders. *Astrophys. J.* **890**, 49 (2020).
28. Dundas, C. M. et al. The formation of gullies on Mars today. *Geolog. Soc. London, Special Publ.* **467**, 67–94 (2019).
29. Hoffman, N. Active polar gullies on Mars and the role of carbon dioxide. *Astrobiology* **2**, 313–323 (2002).
30. Pilorget, C. & Forget, F. Formation of gullies on Mars by debris flows triggered by CO2 sublimation. *Nat. Geosci.* **9**, 65–69 (2016).
31. Bickel, V. T. et al. Deep learning-driven detection and mapping of rockfalls on Mars. *IEEE J. Sel. Topics Appl. Earth Observ. Remote Sens.* **13**, 2831–2841 (2020).
32. Tesson, P.-A. et al. Evidence for thermal-stress-induced rockfalls on Mars impact crater slopes. *Icarus* **342**, 113503 (2020).
33. Grindrod, P. M., Davis, J. M., Conway, S. J. & de Haas, T. Active boulder falls in terra sirenum, mars: Constraints on timing and causes. *Geophys. Res. Lett.* **48**, e2021GL094817 (2021).
34. Sylvest, M. E., Conway, S. J., Patel, M. R., Dixon, J. C. & Barnes, A. Mass wasting triggered by seasonal CO_2 sublimation under Martian atmospheric conditions: Laboratory experiments. *Geophys. Res. Lett.* **43**, 12,363–12,370 (2016).
35. Sylvest, M. E. et al. CO_2 sublimation in Martian gullies: laboratory experiments at varied slope angle and regolith grain sizes. *Geolog. Soc., London, Special Publ.* **467**, 343–371 (2019).
36. Cedillo-Flores, Y., Treiman, A. H., Lasue, J. & Clifford, S. M. CO2 gas fluidization in the initiation and formation of Martian polar gullies. *Geophys. Res. Lett.* **38**, L21202 (2011). https://agupubs.onlinelibrary.wiley.com/doi/abs/10.1029/2011GL049403.
37. Takahashi, T. Debris flow. *Annual Rev. Fluid Mech.* **13**, 57–77 (1981).
38. Iverson, R. M. & LaHusen, R. G. Friction in debris flows: Inferences from large-scale flume experiments. *Hyd. Eng.* **93**, 1604–1609 (1993).
39. de Haas, T., Braat, L., Leuven, J. R. F. W., Lokhorst, I. R. & Kleinhans, M. G. Effects of debris flow composition on runout, depositional mechanisms, and deposit morphology in laboratory experiments. *J. Geophys. Res.: Earth Surf.* **120**, 1949–1972 (2015).
40. Roelofs, L., Colucci, P. & de Haas, T. How debris-flow composition affects bed erosion quantity and mechanisms: An experimental assessment. *Earth Surf. Processes Landforms* **47**, 2151–2169 (2022).
41. Roelofs, L., Nota, E. W., Flipsen, T. C. W., Colucci, P. & de Haas, T. How bed composition affects erosion by debris flows–an experimental assessment. *Geophys. Res. Lett.* **50**, e2023GL103294 (2023).
42. Forget, F. et al. Improved general circulation models of the Martian atmosphere from the surface to above 80 km. *J. Geophys. Res.: Planets* **104**, 24155–24175 (1999).
43. Forget, F. et al. Challenges in Mars climate modelling with the lmd mars global climate model, now called the Mars "PLANETARY CLIMATE MODEL" (PCM). In *Seventh International Workshop on the Mars Atmosphere: Modelling and Observations*, 1102 (2022).
44. Spiga, A. & Forget, F. Fast and accurate estimation of solar irradiance on Martian slopes. *Geophys. Res. Lett.* **35**, L15201 (2008). https://agupubs.onlinelibrary.wiley.com/doi/abs/10.1029/2008GL034956.
45. Vincendon, M. et al. Near-tropical subsurface ice on Mars. *Geophys. Res. Lett.* **37**, L01202 (2010). https://agupubs.onlinelibrary.wiley.com/doi/abs/10.1029/2009GL041426.
46. Lange, L. et al. A reappraisal of subtropical subsurface water ice stability on Mars. *Geophys. Res. Lett*. **50**, e2023GL105177 (2023). https://doi.org/10.1029/2023GL105177.
47. Fergason, R. L., Christensen, P. R. & Kieffer, H. H. High-resolution thermal inertia derived from the Thermal Emission Imaging System (THEMIS): Thermal model and applications. *J. Geophys. Res.: Planets* **111**, E12004 (2006). https://agupubs.onlinelibrary.wiley.com/doi/abs/10.1029/2006JE002735.
48. Edwards, C. et al. Mosaicking of global planetary image datasets: 1. Techniques and data processing for Thermal Emission Imaging System (THEMIS) multi-spectral data. *J. Geophys. Res.: Planets* **116**, E10008 (2011).
49. Pollock, N. M., Brand, B. D., Rowley, P. J., Sarocchi, D. & Sulpizio, R. Inferring pyroclastic density current flow conditions using syn-depositional sedimentary structures. *Bull. Volcanol.* **81**, 1–16 (2019).
50. Smith, G. et al. A bedform phase diagram for dense granular currents. *Nat. Commun.* **11**, 2873 (2020).
51. Scully, J. E. et al. Geomorphological evidence for transient water flow on Vesta. *Earth Planet. Sci. Lett.* **411**, 151–163 (2015).
52. Rothery, D. A. et al. Rationale for BepiColombo studies of Mercury's surface and composition. *Space Sci. Rev.* **216**, 1–46 (2020).

53. Heldmann, J. L. et al. Formation of martian gullies by the action of liquid water flowing under current Martian environmental conditions. *J. Geophys. Res.: Planets* **110**, E05004 (2005). https://agupubs.onlinelibrary.wiley.com/doi/abs/10.1029/2004JE002261.
54. de Haas, T., Åberg, A. S., Walter, F. & Zhang, Z. Deciphering seismic and normal-force fluctuation signatures of debris flows: An experimental assessment of effects of flow composition and dynamics. *Earth Surf. Processes Landf.* **46**, 2195–2210 (2021).
55. Blackburn, D. G., Bryson, K. L., Chevrier, V. F., Roe, L. A. & White, K. F. Sublimation kinetics of CO2 ice on Mars. *Planet. Space Sci.* **58**, 780–791 (2010).
56. Christensen, P. R. et al. Morphology and composition of the surface of Mars: Mars Odyssey THEMIS results. *Science* **300**, 2056–2061 (2003).
57. Diniega, S. et al. Dune-slope activity due to frost and wind throughout the north polar erg, Mars. *Geolog. Soc. London, Spec. Publ.* **467**, 95–114 (2019).
58. Roelofs, L. et al. *Data Supplement to A Theory for Current Mass Flows in Martian Gullies Driven by Carbon Dioxide Sublimation*. Tech. Rep., Utrecht University (2024).

Acknowledgements

LR was supported by the Dutch Research Council (NWO) – grant OCENW.KLEIN.495 to TdH. Experiments were funded by Europlanet – project number 20-EPN-015 to TdH, and partly in-kind by the School of Physical Sciences of the Open University under the leadership of MP. We also acknowledge funding from the CNRS INSU Programme Nationale de Planétologie. We would like to give special thanks to the technicians of the Earth Simulation Laboratory from Utrecht University who helped design and build the flume set-up; Arjan van Eijk, Bas van Dam, Henk Markies and Marcel van Maarseveen. The authors thank the spacecraft and instrument engineering teams for the successful completion and operation of CaSSIS. CaSSIS is a project of the University of Bern funded through the Swiss Space Office via ESA's PRODEX programme. The instrument hardware development was also supported by the Italian Space Agency (ASI) (ASI-INAF agreement no. I/018/12/0), INAF/ Astronomical Observatory of Padova, and the Space Research Center (CBK) in Warsaw. Support from SGF (Budapest), the University of Arizona (LPL), NASA and Manish Patel (UK Space Agency) are also gratefully acknowledged. SJC and KP were supported by a Région Pays de la Loire grant étoiles montantes METAFLOWS (convention N° 2019-14294) and also by the French Space Agency CNES. SRL thanks the UK Space Agency for support under grants ST/W002949/1, ST/R001405/1, ST/T002913/1, and ST/V005332/1.

Author contributions

Design, conduction and analysis of experiments: L.R., T.d.H., S.J.C., M.S., J.M. 1D climate modelling: S.J.C., S.R.L. Satellite data analysis: C.D., S.J.C., K.P., J.R. Paper writing: L.R., S.J.C., T.d.H. Paper editing and reviewing: L.R., S.J.C., T.dH., J.M., C.D., S.R.L., M.P., J.R. Figures: L.R., S.J.C. Acquiring funding and in-kind support: T.dH, S.J.C., M.P. are not compulsory. Where included they should be brief. Grant or contribution numbers may be acknowledged.

Competing interests

The authors declare no competing interests.

Additional information

Supplementary information The online version contains supplementary material available at https://doi.org/10.1038/s43247-024-01298-7.

Correspondence and requests for materials should be addressed to Lonneke Roelofs.

Peer review information : *Communications Earth & Environment* thanks Aditya Khuller, Katherine Auld and Lucas Lange for their contribution to the peer review of this work. Primary Handling Editor: Joe Aslin. A peer review file is available.